Eutrophication model for Lake Washington (USA) Part II—model calibration and system dynamics analysis

George B. Arhonditsis *, Michael T. Brett

Department of Civil and Environmental Engineering, University of Washington, Box 352700, Seattle, WA 98195, USA

Abstract

We developed a complex eutrophication model to simulate the current chemical and biological properties of Lake Washington (USA). The model reproduces the key epilimnetic and hypolimnetic temporal patterns of the system and results in a good fit between simulated and observed monthly values. The relative error of model estimates was below 20% for most of the water quality parameters (phytoplankton, phosphate, total phosphorus, total nitrogen, dissolved oxygen). Discrepancies between simulated and observed ammonium levels were mainly due to the explicitly modeled egestion of excess nitrogen during zooplankton feeding. This indicates that the relation between secondary production and nutrient recycling has significant effects on the fractionation of the major elements (C, N and P) and regulates their distribution between the particulate/dissolved and inorganic/organic pools. The model was forced by 1962 nutrient loadings, when the lake received large quantities of treated wastewater treatment effluent, and accurately predicted the phytoplankton community responses (phytoplankton biomass and cyanobacteria dominance) and the nitrogen and phosphorus annual cycles for these conditions. We used Monte Carlo simulations to reproduce the meteorological forcing (air temperature, solar radiation, precipitation and subsequent river inflows) that in large part regulates phytoplankton interannual variability for the last 25 years in the lake. We found three seasonal components (modes of variability). The first component (January, May, November, December) is associated with the conditions that determine the abundance of the herbivorous cladocerans; the second component (June–September) coincides with the summer-stratified period, and the third component (February–April) is associated with the initiation and peak of the spring bloom. Finally, an illustrative application of two scenarios of nutrient loading increase at 25% of the 1962 levels indicated that both phytoplankton and cyanobacteria growth are likely to be stimulated. The three seasonal components still characterize phytoplankton dynamics, but changes in the relationships between summer phytoplankton/cyanobacteria biomass and total phosphorus/phosphate concentrations indicate the likelihood of structural shifts towards relaxation of the present phosphorus-limiting conditions and promotion of cyanobacteria dominance. Integration of the present eutrophication model with a hydrodynamic model with enhanced vertical resolution will allow more realistic predictions.
© 2005 Elsevier B.V. All rights reserved.

Keywords: Lake management; Eutrophication modeling; Scenarios analysis; Algal food quality

---

 * Corresponding author. Present address: Nicholas School of the Environment and Earth Sciences, Duke University, Durham, NC 27708, USA. Tel.: +1 919 613 8105; fax: +1 919 681 5740.
 E-mail address: georgear@duke.edu (G.B. Arhonditsis).

1. Introduction

The concept of model validation has been extensively debated during the last three decades, and the ecological literature is replete with contradictory viewpoints about the feasibility or even the definition of model validation (Van Horn, 1971; Caswell, 1976; Holling, 1978; Oreskes et al., 1994; Rykiel, 1996). For example, Oreskes et al. (1994) claimed models which attempt to reproduce open natural systems can never be validated. This paper also questioned the adequacy of environmental models for public policy decision-making and claimed earth science models have only heuristic value. At the other end of the spectrum, some authors consider model validation to be a mere technical process that aims to determining the level of agreement between the model and an independent data-set obtained from a real system (Goodall, 1972; Mayer and Butler, 1993; Power, 1993). Rykiel (1996) argued that there are "semantic and philosophical considerations" that cause this confusion, but also emphasized the lack of universal validation tests and standards as another source of ambiguity for the whole modeling procedure. Most importantly, he emphasized the need for modelers to clearly specify the model objectives, explicitly state what they consider to be acceptable model behavior and to define the model operational domain. Undoubtedly, there are both subjective and objective aspects of the validation process that confuse its meaning, while this confusion is accentuated by the often times dual nature of environmental models in scientific hypothesis testing and engineering practice (Caswell, 1988).

In aquatic science, there are simulation models that have been developed for theoretical purposes in order to explore aspects of system dynamics that are technologically or economically unattainable by other means (Franks, 1995). These theoretical models also provide a foundation from which one can analyze chemical or trophic dynamics (Norberg and DeAngelis, 1997), test new ecological theories for aquatic systems (Jorgensen, 1995), couple physical processes with biological dynamics (Kamykowski et al., 1994) or study their transition towards chaotic behavior (Rinaldi and Muratori, 1993; Scheffer et al., 2000). The second category, which is not always mutually exclusive with the previous theoretical class, includes models that have been constructed for management and forecasting purposes. The performance of these models is constrained by

available data, and they are used as heuristic tools to identify the underlying dynamics of the system behavior or as predictive tools to explore hypothetical conditions that are not described by current observations. As Franks (1995) pointed out the former class of models interpolate within the data, while the later extrapolate beyond the data. In the aquatic ecosystems literature, there are numerous references to models that have been used for understanding oceanic ecosystems (e.g., bloom dynamics, the global carbon cycle) and predicting biotic responses to climate change (Fasham et al., 1993; Frost and Kishi, 1999; Boyd and Doney, 2002; Kawamiya, 2002), but this class of models has also been used as management tools for predicting eutrophication or integrating environmental with socioeconomic concerns (Ambrose et al., 1991; Cerco and Cole, 1994; Hamilton and Schladow, 1997; Turner, 2000; Arhonditsis et al., 2000, 2002).

Based on the previous classification, the eutrophication model that we presented in Part I can serve both theoretical and practical engineering/management purposes. For example, we introduced a dynamic parameterization for modeling the effects of both food quality and quantity on zooplankton gross growth efficiency, and also used a multi-elemental approach that makes it possible to examine recent conceptual advances in stoichiometric nutrient recycling theory. In this sense, our model was used for addressing questions of the type "*What would happen if . . .?*", which in turn identified components of the system that require further research (Franks, 1995). At the same time, the basic goal for the development of this biogeochemical model is to support management-planners and decision-makers as a methodological tool for testing Lake Washington's resilience under various management scenarios. Therefore, our model evaluation was based on the calibration and validation processes, as they were defined in a "limited technical sense" by Rykiel (1996). During calibration, we attempted to obtain a "sufficient" description of the lake's mean annual patterns by adjustment and estimation of model parameters and constants. Inevitably, given the lack of conventional and widely accepted standards of model performance, the characterization "sufficient" entails some subjectivity. However, goodness-of-fit assessments were based on commonly applied diagnostic measures in modeling practice (Mayer and Butler, 1993; Power, 1993), and thus the performance of our model can be compared

with similar studies. We also considered two components of the validation process, the conceptual and operational validation. The former aims to provide justification for the formulations used and the rationale for the simplifications adopted and was extensively discussed in Part I. The later examines the engineering value of the model and demonstrates whether the model outputs meet the performance standards required for the model's ultimate management purpose. [Note that here we distinguish between model calibration and operational validation.] As a part of the operational validation of the model, we explored the simulated internal structure of the system (i.e., "structural validation" sensu Ziegler, 1976), and assessed its correspondence with the actual processes or cause-effect relationships reported in the Lake Washington literature. In addition, since the model's intended application is for predictive purposes, we included a series of perturbations (nutrient loading, meteorological forcing) that reproduced past, current and future hypothesized states for this system. The model showed a satisfactory behavior and produced realistic patterns. Ironically the present model structure is not directly comparable with past conditions in Lake Washington, because during that period *Daphnia* was not a prominent member of the zooplankton community. This supports the notion that simulation models cannot replicate the enormous complexity of natural systems (Reckhow, 1999), and thus the modeling procedure should be considered an iterative process where model formulation and validation criteria always evolve in a parallel manner with the real system (Rykiel, 1996). Finally, this paper emphasizes the need for integrating the present eutrophication model with a hydrodynamic model having a fine vertical resolution, and suggests aspects of Lake Washington dynamics that should be incorporated into future monitoring programs.

2. Model application and calibration results

The data-set used for model calibration was collected on a bi-weekly (during the summer) or monthly (the rest of the year) basis from 12 inshore and offshore sampling stations from January 1995 to December 2001 (Arhonditsis et al., 2003, Fig. 1). The environmental variables monitored included chlorophyll a, phosphate, total phosphorus, nitrate, ammonium, total nitrogen, dissolved oxygen and total organic carbon. The data were binned by month based on time-weighted averages — bi-weekly or monthly field measurements were linearly interpolated and the resulting daily time series were averaged over the months. Epilimnetic and hypolimnetic volume weighted averages were calculated using lake morphometric data (Edmondson and Lehman, 1981), and the depths defining the range of the two spatial compartments were consistent with the model physical segmentation. Silica concentrations reported from 1986 to 1992 and a long time-series of zooplankton data (1975–1999) were also used for model calibration (Edmondson, 1997; Scheuerell et al., 2002). The carbon per volume conversion for each zooplankton group was based on length–weight relationships provided by Downing and Rigler (1984) and a mean carbon mass to dry weight ratio of 45%.

The eutrophication model was calibrated by tuning the model parameters within their observed literature ranges, as derived and used in the model sensitivity analysis. The parameter values found to give the best fit between simulated data and the lake's mean annual patterns are reported in Appendix B of Part I. The comparison between simulated and observed values for Lake Washington's epilimnion and hypolimnion is shown in Figs. 1 and 2. It can be seen that the model provides a reasonable reproduction of the mean annual epilimnetic patterns for zooplankton biomass, chlorophyll a, phosphate, total phosphorus, total nitrogen, nitrate, dissolved oxygen and total organic carbon concentrations. However, major discrepancies exist between the observed and simulated ammonium concentrations. During most of the annual cycle the model results in very low ammonium concentrations ($\leq 10 \, \mu g \, l^{-1}$), which contrast with the observed values which range from 20 to $30 \, \mu g \, l^{-1}$ range. In addition, the model silica cycle has a smoother transition from the winter maxima ($\approx 2 \, mg \, l^{-1}$) to the spring minima and overestimates summer values. The predicted hypolimnetic annual chlorophyll cycle is in agreement with the observed data, with the only exception being the late spring (May–June) concentrations when the model predicts a more rapid phytoplankton biomass decline. Total phosphorus, total nitrate, dissolved oxygen and total organic carbon dynamics in the hypolimnion are also accurately simulated. Lake Washington summer nitrate levels ($\approx 240 \, \mu g \, l^{-1}$) are underestimated
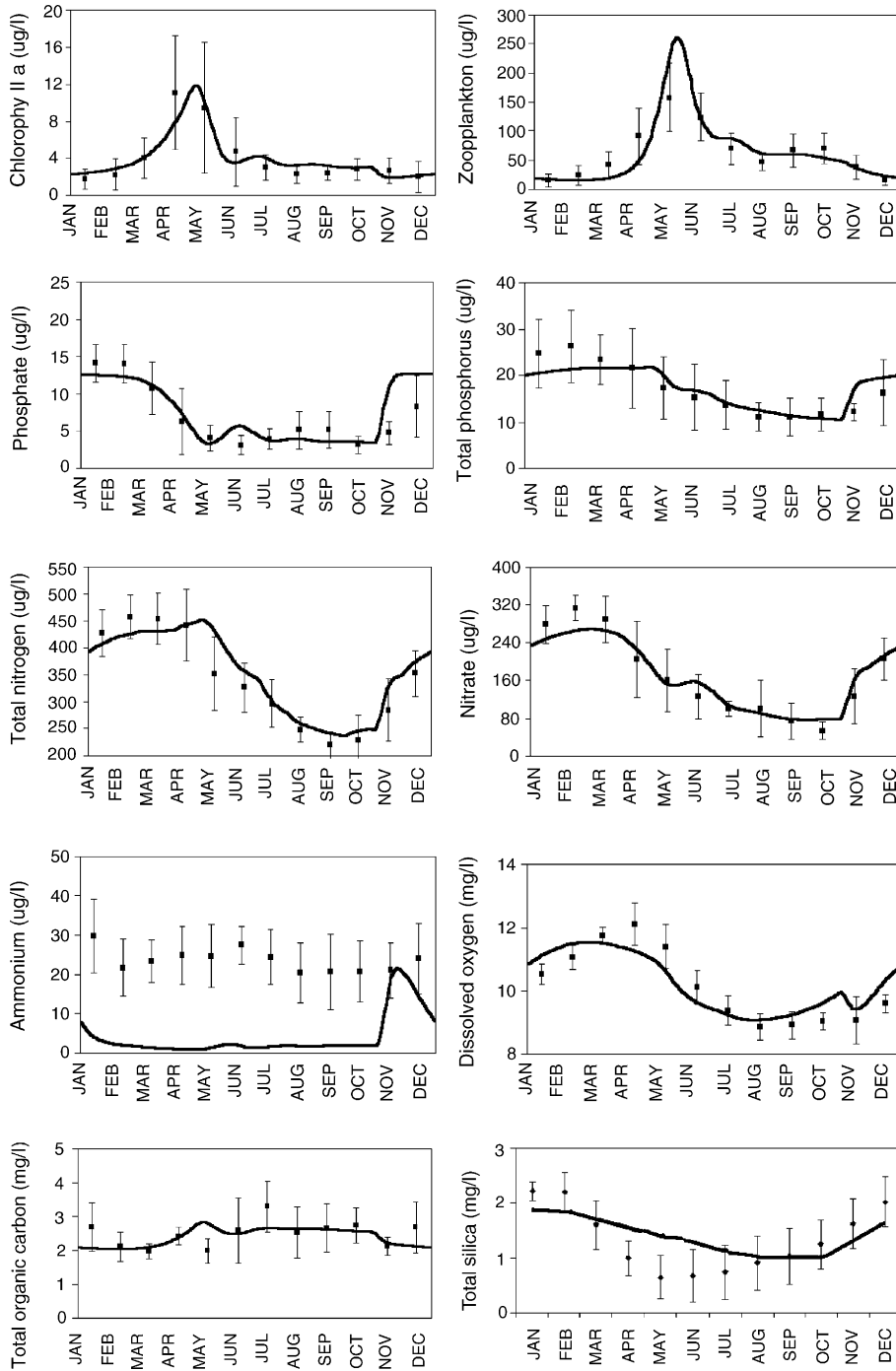
Fig. 1. Comparison between simulated and observed values for Lake Washington epilimnion. The dots correspond to the mean volume weighted averages, while the error bars represent the standard deviations for the monthly parameter values for all stations and years (1995–2001) in the King County monitoring program.
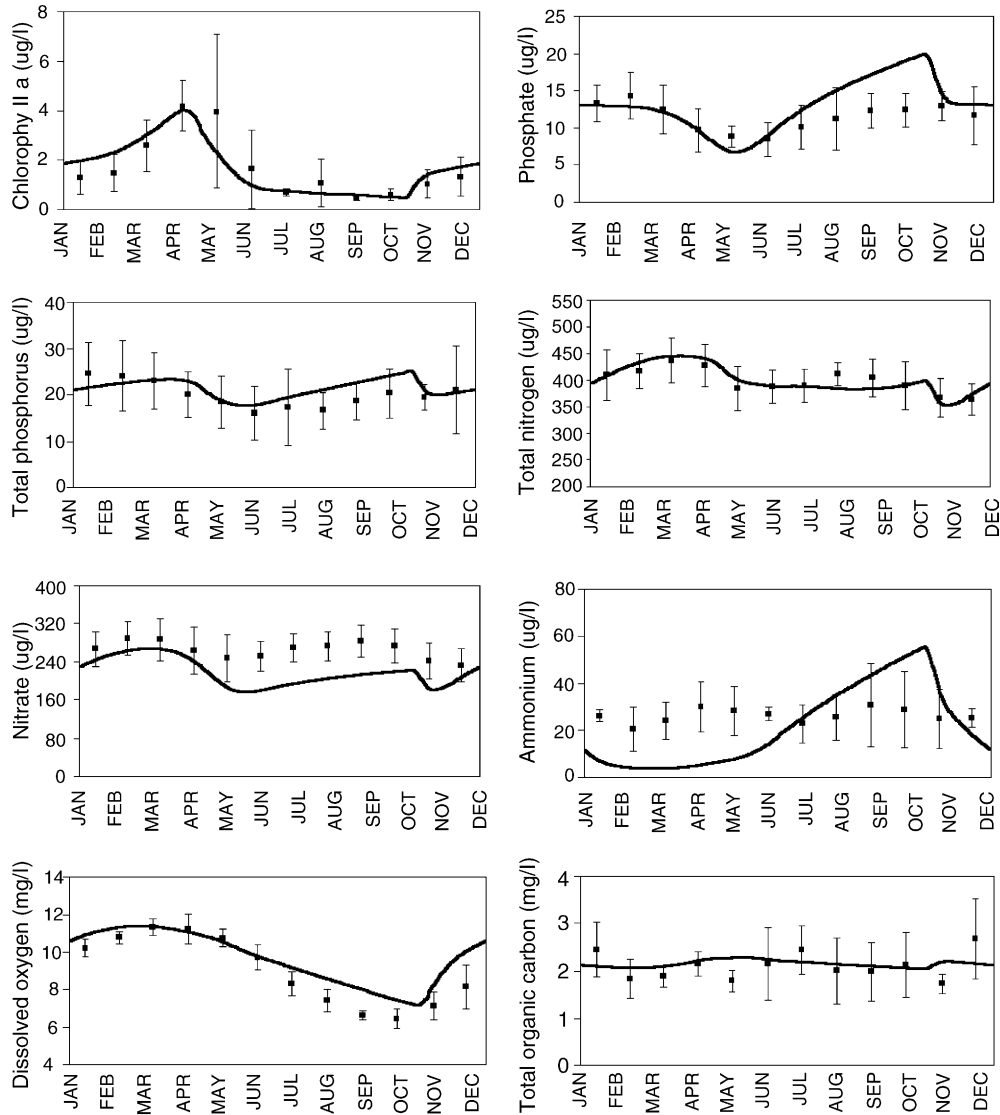
Fig. 2. Comparison between simulated and observed values for Lake Washington hypolimnion. The dots correspond to the mean volume weighted averages, while the error bars represent the standard deviations for the monthly parameter values for all stations and years (1995–2001) in the King County monitoring program.

by the model (160–180 μg l^{-1}). Moreover, the model predicts higher hypolimnetic phosphate ($\approx$20 μg l^{-1}) and ammonium ($\approx$50 μg l^{-1}) accumulation during the stratified period, than what is actually observed in the lake. Fig. 3 shows the plankton succession patterns as simulated by the model. During the spring bloom, the dominant phytoplankton taxa predicted by the model are diatoms (55% of the total phytoplankton biomass),

with greens and cyanobacteria accounting for 33% and 18%, respectively. In contrast, the summer phytoplankton community is divided almost equally between these three groups. Both results are very close to typical patterns in Lake Washington, in its post-recovery from severe eutrophication phase (Arhonditsis et al., 2003). The model also describes the zooplankton annual cycle, with copepod dominance until May
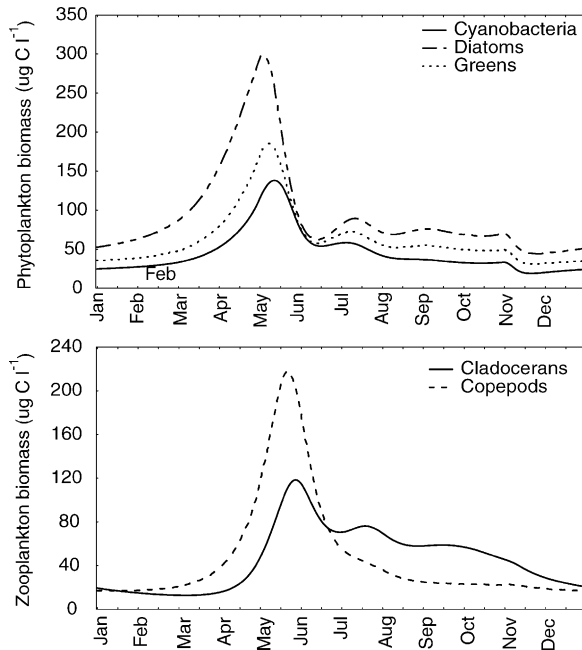
Fig. 3. Seasonal phytoplankton and zooplankton succession patterns as simulated by the model.

and cladoreran dominance during the summer and fall.

Table 1 presents an assessment of the goodness-of-fit between the simulated and observed monthly values

for the Lake Washington epilimnion, hypolimnion and overall lake volume. We used three diagnostic measures for this quantification: the mean error, the relative error and the coefficient of determination. The mean error (ME) is calculated as $\sum$(observed value − simulated value)/number of observations, and is a measure of model bias which should be close to zero (Power, 1993). The relative error (RE) characterizes model accuracy and is calculated as $\sum$ |observed value − simulated value| / $\sum$ observed value. The coefficient of determination (r^2) is a statistical measure commonly used in model evaluation (Mayer and Butler, 1993). Satisfactory agreement is obtained for the epilimnetic (ME = 0.01 $\mu g\,l^{-1}$, RE = 20%, r^2 = 0.91) and overall lake volume (ME = −0.38 $\mu g\,l^{-1}$, RE = 22%, r^2 = 0.93) chlorophyll levels, while the high hypolimnetic ME (−2.32 $\mu g\,l^{-1}$) and RE (137%) values result from the previously mentioned late spring-early summer discrepancies. Generally, a fairly low bias and high accuracy characterizes the model predictions for zooplankton abundance, dissolved oxygen, total nitrogen, total phosphorus, phosphate, and silica concentrations. The lower r^2 values for the hypolimnion are largely a statistical artifact, because there is much less annual variability to be explained in these data. This is also true for the total organic carbon concentrations (r^2 < 0.10), since both the ME

Table 1

Goodness-of-fit statistics for the Lake Washington eutrophication model, based on the monthly values (1995–2000) of dissolved oxygen (DO), total nitrogen (TN), nitrate (NO_3), ammonium (NH_4), total phosphorus (TP), phosphate (PO_4), chlorophyll a (chla), total organic carbon (TOC), total zooplankton biomass (ZOOP), and total epilimnetic silica (Si)

	DO (mg/l)	TN (μg/l)	NO$_3$ (μg/l)	NH$_4$ (μg/l)	TP (μg/l)	PO$_4$ (μg/l)	chla (μg/l)	TOC (mg/l)	ZOOP (μg/l)	Si (mg/l)
Epilimnion										
Mean error	−0.09	−12.10	0.40	19.74	−0.10	−0.53	0.01	0.08	−1.61	−0.07
Relative error	5%	7%	11%	84%	12%	23%	20%	11%	25%	27%
r^2	0.77	0.90	0.95	0.01	0.79	0.71	0.91	0.10	0.88	0.49
Hypolimnion										
Mean error	−1.23	46.67	95.33	22.12	2.76	4.06	−2.32	−0.30		
Relative error	14%	15%	36%	85%	17%	37%	137%	21%		
r^2	0.91	0.72	0.43	0.10	0.32	0.43	0.69	0.00		
Water column[a]										
Mean error	−0.47	3.39	33.98	15.65	0.03	0.07	−0.38	−0.03		
Relative error	7%	5%	16%	65%	8%	15%	22%	12%		
r^2	0.86	0.85	0.89	0.07	0.79	0.68	0.93	0.02		

Details about the sampling network are provided in Arhonditsis et al. (2003).

[a] Averages weighted over the epilimnion and hypolimnion volume.

(-0.30–0.08 mg l^{-1}) and RE (11–21%) values are satisfactory. A good agreement is obtained between the simulated and observed epilimnetic nitrate concentrations (ME = 0.40 μg l^{-1}, RE = 11%, r^2 = 0.95). However, model agreement notably decreases in the hypolimnion (ME = 95.33 μg l^{-1}, RE = 36%, r^2 = 0.43) due to the previously mentioned summer nitrate underestimation. This also affects the overall lake results for nitrate (ME = 33.98 μg l^{-1}, RE = 16%, r^2 = 0.89). Based on the results of an individual state-variable performance assessment by Arhonditsis and Brett (2004, see their Fig. 3 and Table 1), we infer that the fit for all the state variables (overall, epilimnion and hypolimnion) is above the top 30th percentile for this class of models. In contrast, ammonium is the most poorly predicted state-variable with fairly high ME (>15 μg l^{-1}), while both the RE (>65%) and r^2 (<0.10) values were lying below the 50% percentile of the same study's reported ammonium performance (Arhonditsis and Brett, 2004).

3. Lake Washington dynamics: simulated and observed fluxes

3.1. Nitrogen and phosphorus budgets

The simulated annual nitrogen and phosphorus cycles for the epilimnion and hypolimnion are presented in Figs. 4 and 5. As mentioned in Part I, external loading was based on mean annual nutrient cycles over the past 10 years for all important Lake Washington tributaries (Brett et al., in press). The model considers an annual hydrologic loading of 1152×10^6 m^3 year^{-1} from fluvial and aerial sources. After a correction for evaporative losses at the lake surface, these inputs correspond to a hydraulic renewal rate of 0.384 year^{-1}. Both fluvial and atmospheric total nitrogen inputs supply 1114×10^3 kg year^{-1}, and nitrate and ammonium loading supplies are 561 and 34×10^3 kg year^{-1}, respectively. Moreover, the system losses 397, 238 and 12×10^3 kg year^{-1} of total nitrogen, nitrate and ammonium respectively through the Lake Union Ship Canal outflow. The exogenous total phosphorus loading contributes approximately 74.9×10^3 kg year^{-1}, while 23.9 and 17.3×10^3 kg year^{-1} entering the system as dissolved phosphorus and phosphate. After accounting for the outflows, the respective net annual inputs

are 56.4, 7.8 and 6.4×10^3 kg year^{-1}. According to the model outputs, the net phytoplankton growth (uptake minus basal metabolism) utilizes 677×10^3 kg year^{-1} of nitrogen and 47×10^3 kg year^{-1} of phosphorus. Zooplankton consumes 596×10^3 kg year^{-1} of nitrogen and 54×10^3 kg year^{-1} of phosphorus through phytoplankton grazing. Detrivory also accounts for 1020 and 83×10^3 kg year^{-1} of nitrogen and phosphorus, respectively. Both egestion of the unassimilated material and zooplankton basal metabolism recycle 1264×10^3 kg year^{-1} of nitrogen and 99×10^3 kg year^{-1} of phosphorus. Finally, the annual fluxes of nitrogen and phosphorus to the sediments are 741 and 65×10^3 kg year^{-1}, while 456 and 46×10^3 kg year^{-1} of the nitrogen and phosphorus sedimenting particulate debris is regenerated in the water column or the sediments.

3.2. Nutrient recycling and sedimentation rates

The inclusion of an independent adjustment of zooplankton C, N and P efficiencies, which kept somatic elemental ratios constant, increased model sensitivity to non-limiting elemental recycling. According to stoichiometric theory, both grazer and food elemental composition influence nutrient release rates and ratios. In addition, stoichiometric theory predicts that zooplankton with low body C:P and N:P ratios recycle nutrients at higher C:P and N:P ratios than zooplankton taxa with high somatic C:P and N:P ratios (Elser and Urabe, 1999). The zooplankton C:N:P stoichiometries (by weight) used in the model were 35:5.8:1 for cladocerans and 50:10:1 for copepods. Based on the model consideration that both prior assigned preferences and relative concentrations of the four food-types determine zooplankton selectivity, the mean annual elemental composition of the food ingested was 58:12:1 for cladocerans and 58:11:1 for copepods. Consequently, the elemental ratios of egested unassimilated material were 77:17:1 for the P-rich cladocerans and 64:11:1 for the N-rich copepods. When using quantities, these ratios are interpreted as 5692 and 1064×10^3 kg year^{-1} of excess carbon and nitrogen during zooplankton feeding and correspond to 83% [egestion: (egestion + basal metabolism)] of zooplankton recycling in the system. During calibration, we assumed the same particulate/dissolved and inorganic/organic fractionation for both plankton basal metabolism and zooplankton
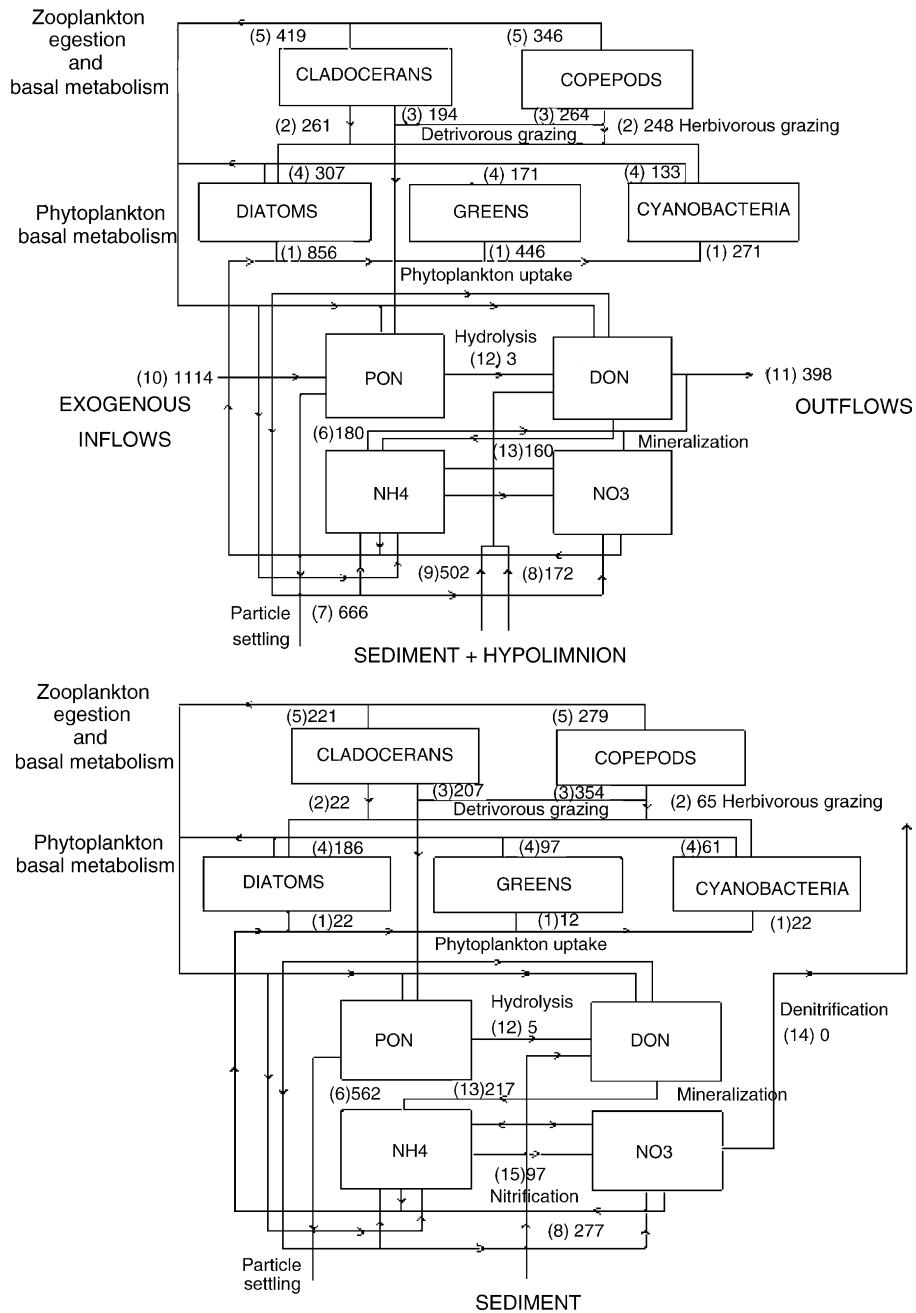
Fig. 4. Annual epilimnetic and hypolimnetic nitrogen fluxes. The simulated processes are: (1) phytoplankton uptake, (2) herbivorous grazing, (3) detrivorous grazing, (4) phytoplankton basal metabolism excreted as NH_4, DON and PON, (5) NH_4, DON and PON excreted by zooplankton basal metabolism or egested during zooplankton feeding, (6) settling of particulate nitrogen on the sediment, (7) settling of particulate nitrogen in the hypolimnion, (8) water-sediment NO_3, NH_4 and DON exchanges, (9) fluxes from the hypolimnion, (10) exogenous inflows of NO_3, NH_4, DON and PON, (11) outflows of NO_3, NH_4, DON and PON to Puget Sound, (12) PON hydrolysis, (13) DON mineralization, (14) NO_3 sinks due to denitrification, (15) nitrification. The unit is 10^3 kg year^{-1}.
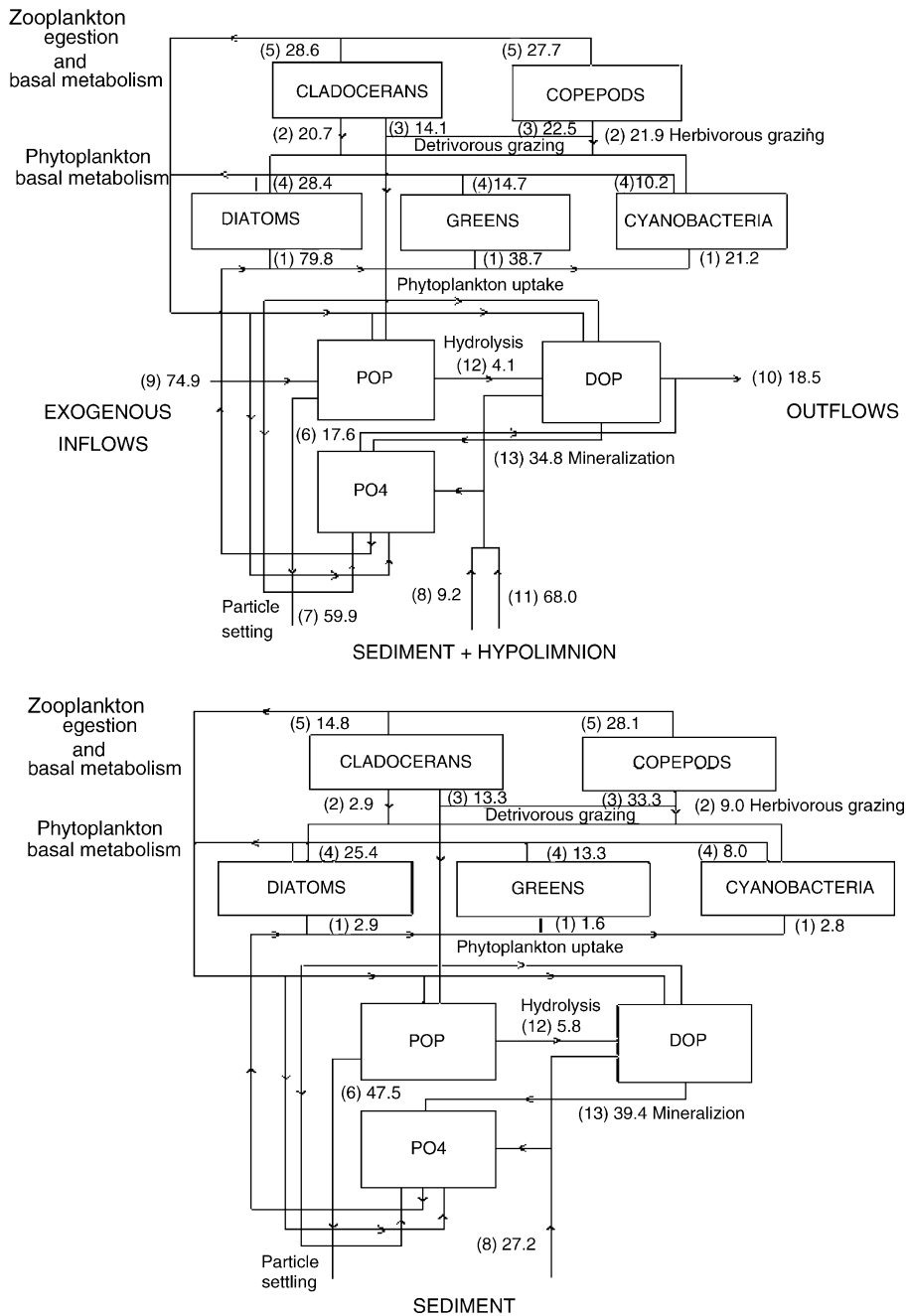
Fig. 5. Annual epilimnetic and hypolimnetic phosphorus fluxes. The simulated processes are: (1) phytoplankton uptake, (2) herbivorous grazing, (3) detrivorous grazing, (4) phytoplankton basal metabolism excreted as PO_4, DOP and POP, (5) PO_4, DOP and POP, excreted by zooplankton basal metabolism or egested during zooplankton feeding, (6) settling of particulate phosphorus on the sediment, (7) settling of particulate phosphorus in the hypolimnion, (8) water-sediment PO_4 and DOP exchanges, (9) exogenous inflows of PO_4, DOP and POP, (10) outflows of PO_4, DOP and POP to Puget Sound, (11) fluxes from the hypolimnion, (12) POP hydrolysis, (13) DOP mineralization. The unit is $10^3 \, kg \, year^{-1}$.

egestion. We found that the assignment of higher values to the dissolved nitrogen fraction, greatly increased ammonium levels and particularly enhanced summer hypolimnetic accumulation. These results reflect the stoichiometric theory prediction that if homeostasis is maintained via post-assimilation processing and differential excretion of nutrients in dissolved form, then zooplankton recycling will tend to increase the retention time of the non-limiting elements in the water column (Elser and Foster, 1998). One way to tackle this problem is to increase nitrification rates, which was also suggested as a possible explanation for nitrate accumulation in Lake Washington's hypolimnion (Lehman, 1988). However, this was achieved by assigning nitrification rates ($>0.2\,\mathrm{mg\,N\,m^{-3}\,day^{-1}}$) which were higher than rates previously observed in eutrophic lakes (Gelda et al., 2000). Hence, the present model calibration apportions the majority of the recycled nitrogen to the particulate fraction (65%), while the implied system conceptualization is depicted in Fig. 6. The resulting model nitrogen sedimentation rates varied between 0.5 and $1.4\,\mathrm{g\,m^{-2}\,month^{-1}}$. Edmondson and Lehman (1981) found similar rates using sediment traps during a 6-year period from April 1971 to December 1977. It should be noted however that only the last two years of this period coincide with the *Daphnia* resurgence in Lake Washington, which is likely to have caused increased nitrogen sedimentation. A careful inspection of Fig. 9 of Edmondson and Lehman (1981) (both the sediment trap measurements and their budget calculations) does not show changes in the sedimentation ranges (maximum and minimum values) over these two years but does show a more uniform intraannual deposition. The model's net nitrogen flux to the sediments varies from -0.12 to $0.8\,\mathrm{g\,m^{-2}\,month^{-1}}$, while the ammonium and nitrate release from the sediments are in good agreement with past studies of this lake (Devol, pers. comm.; Kuivila and Murray, 1984).

The model's carbon recycling fractionation also stems from the findings of Quay et al. (1986). It was pointed out that most of the primary production ($>50\%$) was recycled in the epilimnion and a smaller fraction, about a third, sedimented to the hypolimnion. The model's epilimnetic POC fluxes were $0.87 \times 10^6\,\mathrm{mol\,C\,day^{-1}}$ on average and were very close to the measurements of Quay et al. (1986) ($0.91 \pm 0.13 \times 10^6\,\mathrm{mol\,C\,day^{-1}}$). In addition, the model's mean carbon deposition rate to the sed-
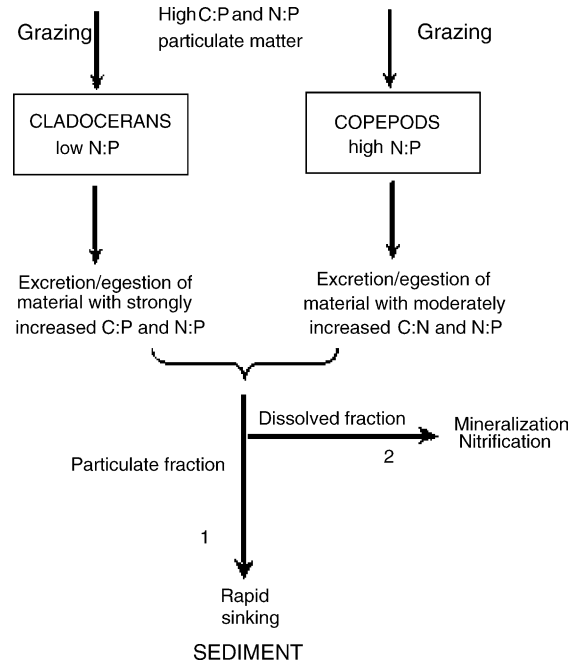

Fig. 6. Conceptual model of the zooplankton elemental composition effects on the N:P ratio of the excreted/egested material. During calibration, the assignment of higher values to the dissolved nitrogen fraction (arrow 2), greatly increased ammonium levels and particularly enhanced summer hypolimnetic accumulation. These results reflect the stoichiometric theory prediction that if homeostasis is maintained via post-assimilation processing and differential excretion of nutrients in dissolved form, then zooplankton recycling will tend to increase the retention time of the non-limiting elements in the water column (Elser and Foster, 1998). In this study, the most effective calibration strategy was to apportion the majority of the recycled nitrogen to the particulate fraction (arrow 1). This partitioning corresponds to the hypothesis that zooplankton homeostasis is also maintained during the digestion and assimilation process, i.e., by removing elements in closer proportion to zooplankton body ratios than to the elemental ratio of the food.

iments was about $0.12\,\mathrm{g\,m^{-2}\,day^{-1}}$, which is similar to the Kuivila and Murray (1984) estimate of $0.15\,\mathrm{g\,m^{-2}\,day^{-1}}$. Based on the model's sedimentation and burial rates used by Kuivila et al. (1988), we found a mean annual sediment oxygen consumption of $232\,\mathrm{mg\,m^{-2}\,day^{-1}}$ which lies within the measured range of $135–280\,\mathrm{mg\,m^{-2}\,day^{-1}}$ by the same study. The simulated sedimentation rates and net fluxes of phosphorus to the sediments vary from 0.04 to 0.12 and 0.02 to $0.06\,\mathrm{g\,m^{-2}\,month^{-1}}$, respectively. Moreover, mean annual phosphorus releases from the sediments are $38\,\mathrm{mg\,m^{-2}\,month^{-1}}$ and account for about 55% of

the gross phosphorus deposition to surficial sediments (Edmondson and Lehman, 1981; Lehman, 1988). According to the model, the N:P ratio (by weight) of the sedimenting material is 11 and lies between the budget (12.74) and sediment trap (6.52) estimates of Edmondson and Lehman (1981). Finally, it should be pointed out that the present calibration minimizes nitrogen hydrolysis and mineralization in the water column and considers a uniform settling velocity for all particulate material. An alternative – more complex – strategy would have been to adopt a model that distinguishes between the rapidly sinking (and therefore unmodified by bacterial processing) zooplankton egesta and the more slow sinking and readily scavenged phytoplankton and detrital material (Elser and Foster, 1998, Fig. 2).

3.3. Simulated Lake Washington seasonal patterns

During the winter period, low surface irradiance (<200 Langleys day^{-1}), short day length (<9 h), and especially greater water column mixing (i.e., a greater epilimnion depth) impose strong light limitation ($f_{\text{light}(i)} \approx 0.1$–0.2) on phytoplankton growth. The model's primary production rates vary around 100 mg C m^{-2} day^{-1}, which is similar to field measurements in Lake Washington (Devol and Packard, 1978; Quay et al., 1986). Low food concentrations and temperature limitation (especially for cladocerans with $f_{\text{temperature}(\text{clad})} < 0.2$) also control zooplankton abundance. The wider temperature tolerance of copepods ($f_{\text{temperature}(\text{cop})} \approx 0.8$) along with their higher feeding rates ($KZ_{(\text{cop})} < KZ_{(\text{clad})}$) at low food levels allows them to dominate the winter zooplankton community. Therefore, copepods respond to the initiation of the spring bloom and reach their maximum abundance ($\approx 200\ \mu g\ C\ l^{-1}$) by the end of May. Development of the model's spring phytoplankton bloom is based on two driving forces, i.e., increased light availability ($f_{\text{light}(i)} > 0.2$) and the onset of thermal stratification. The latter was obtained by progressively lowering the March diffusivity values (<50 m^2 day^{-1}) and reducing the epilimnion depth. Since diatoms have both affinity (growth$_{\text{max}(i)}$/KP$_{(i)}$) and velocity (growth$_{\text{max}(i)}$) advantages as phosphorus competitors and also have lower temperature optima, they dominate the spring phytoplankton community. The maximum phytoplankton biomass (>10 μg chla l^{-1}) occurs in the mid-May, and by this time the system becomes phosphorus lim-

ited ($f_{\text{phosphorus}(i)} < 0.25$). Meanwhile, cladoceran temperature limitation is lessened ($T_{(\text{epi})} \geq 10\,^{\circ}\text{C}$) and their higher maximum grazing rates allow them to dominate the summer zooplankton community. Fig. 7 shows the simulated epilimnetic phosphorus fluxes in Lake Washington during the stratified period. The net phosphorus input from exogenous sources to the system is 10.3×10^3 kg with 32% entering in the form of readily available phosphate. Net phytoplankton production takes up 16.9×10^3 kg, while zooplankton sequesters 11.7 and 7.7×10^3 kg of phosphorus through herbivory and detrivory. According to the model, the downward epilimnetic particulate organic phosphorus flux accounts for 20.2×10^3 kg, while phosphorus (phosphate and dissolved organic phosphorus) intrusion from the hypolimnion is estimated to be 3.9×10^3 kg. This vertical transport is higher than the mean estimate of 0.0148 mg m^{-2} day^{-1} by Lehman (1978), but still is much smaller compared to other epilimnetic sources. For example, phosphorus recycling contributes 14.3×10^3 kg and if we associate these fluxes with zooplankton egestion and basal metabolism (especially for cladocerans), we can infer that a high proportion of the phytoplankton phosphorus demands in the mixed layer are met by zooplankton nutrient recycling. This conclusion is similar to the findings of past studies for this lake (Lehman, 1978; Richey, 1979). During the period from June to October, fish predation consumes on average about 300×10^3 kg month^{-1} of zooplankton (wet weight), which is also in accordance with bioenergetic simulations of planktivorous fishes in Lake Washington (Beauchamp, 1996). Based on both food quality and quantity, zooplankton gross growth efficiencies have their lowest values during the winter period (0.35–0.4), highest values during the spring bloom (>0.6) and vary within a fairly narrow range (0.45–0.5) during the summer-stratified period. These values are at the high end of the literature reported values for herbivorous zooplankton (Straile, 1997), which reflects the generally favorable biochemical composition of seston in Lake Washington vis-à-vis zooplankton nutritional demands (Ballantyne et al., submitted for publication). The ability of copepods to actively select favorable food results in their diet consisting of less than 5% of cyanobacteria. Diatoms and detritus each contribute about 35–40% to copepod diets, while green algae account for the remaining 20% during the summer period. In addition, detritus dominates
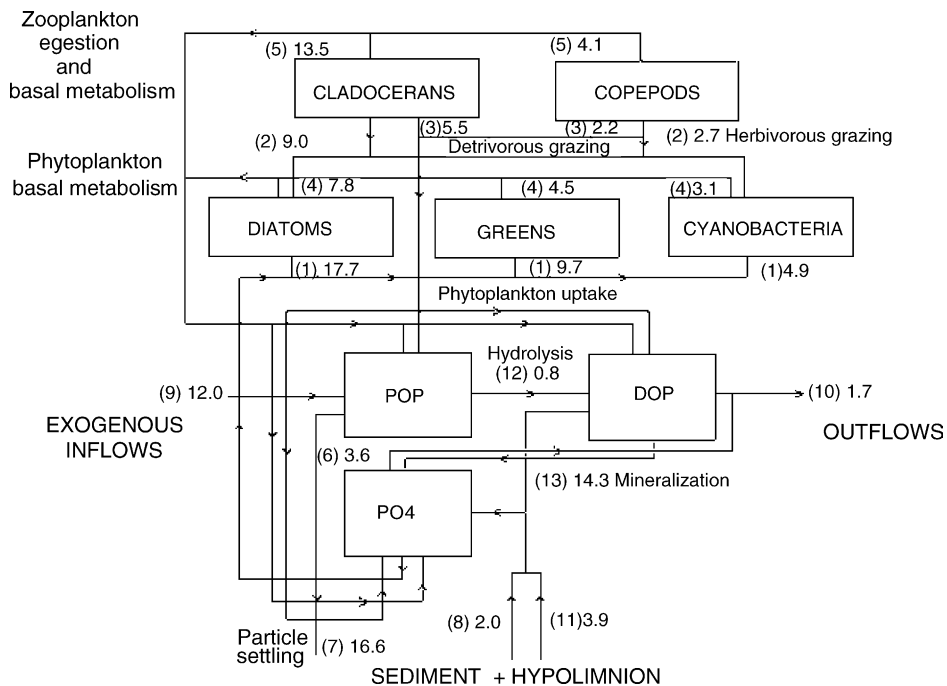
Fig. 7. Total phosphorus fluxes during the stratified period. The unit is 10^3 kg. (The numbers denote the same processes with those of Fig. 5.)

the copepod diets during the winter period ($\approx 80\%$) when phytoplankton biomass is low. Diatoms account for 60% of the ingested food during the spring bloom. Cladocerans were modeled as filter-feeders with equal nominal preferences and a food selection ability driven by the relative availability of the four food-types at any given time. Therefore, similar patterns were observed for diatom and detritus consumption indicating that food abundance is the main factor that determines zooplankton food selectivity. The main diet difference between copepods and cladocerans involved cyanobacteria, which accounted for as much as 20% of clado-cerans diet during the stratified period.

4. Model performance under increased nutrient loading

One of the most desirable properties of an eutrophication model is its capability to predict how the system will respond to changes in external forces such as nutrient loading. Power (1993) described this procedure as the predictive validation of the model, which basically assesses the model-fit with independent data sets or data acquired from the real system after model calibration. A common modeling practice is to split the available data into two subsets, and use the first for calibrating the model and the second for testing its predictive ability (e.g., Schladow and Hamilton, 1997). However, if the second subset does not describe conditions that differ significantly from those used during the calibration, then the validation steps may not confirm whether the model can predict responses to new driving forces (Omlin et al., 2001). Lake Washington provides an excellent case for testing a model's robustness in its extrapolation domain, since it was studied extensively during the past 40 years during which time nutrient loading varied greatly. The existing data cover a wide range of nutrient loading conditions, i.e., the period when the wastewater effluents were diverted from the lake (1963–1968), the transient phase (1969–1974), and current conditions (Edmondson, 1997). In Part I, it was shown that the model is particularly sensitive to external nutrient loading, which accounted for most of the phytoplankton and cyanobacteria variability. This analysis was based on perturbations that reproduced external loading interannual variability during current conditions, and was mostly driven by meteorological

forcing via river inflows. Hence, this test only verified that the model could simulate individual years within the present Lake Washington post-eutrophication and *Daphnia* resurgence phase (Edmondson, 1994), and indeed, the model successfully simulated the years 1995–1997 (not presented in this paper). However, it does not provide insights into how the model would respond to nutrient enrichment similar to what Lake Washington experienced with the quantitative and qualitative characteristics of sewage discharges during the pre-wastewater diversion period.

4.1. Simulation of the 1962 nutrient loading conditions

We tested the model's performance (with the parameter values listed in Appendices A and B, Part I) relative to 1962 nutrient loading conditions, because during this year Lake Washington received the maximum input of treated sewage effluent (Edmondson and Lehman, 1981, Tables 6–10). Thus, this year represents the most extreme enrichment conditions previously encountered by the lake. However it should be noted that the structure of the present eutrophication model is not directly compatible with the prediversion years, because during that period *Daphnia* was not a prominent component of the zooplankton community. *Daphnia* was established after 1976 as a result of bottom-up (due to the disappearance of the filamentous cyanobacterium i.e., *Oscillatoria*) and top-down (due to reduced predation by mysid shrimp) biotic control (Edmondson, 1994). Hence, we tested the model twice against the 1962 nutrient loading scenario. The first time after deactivating the cladoceran group, and the second using the full model structure. Fig. 8 shows the model results without cladocerans, which was most similar to 1962 Lake Washington plankton community. The model predicted a chlorophyll annual cycle with a maximum of 38 μg l^{-1} and mean summer concentrations of 10 μg l^{-1}. In addition, cyanobacteria became the predominant phytoplankton group with their proportion of total phytoplankton varying between 30 and 95% during the year. Total nitrogen, total phosphorus and phosphate levels were also fairly close to those reported by Edmondson and Lehman (1981, see their Table 11). The model consistently underestimated nitrate levels (ME $\approx$ 150 μg l^{-1}), while the summer ammonium levels were about 20–30 μg l^{-1} higher than the observed
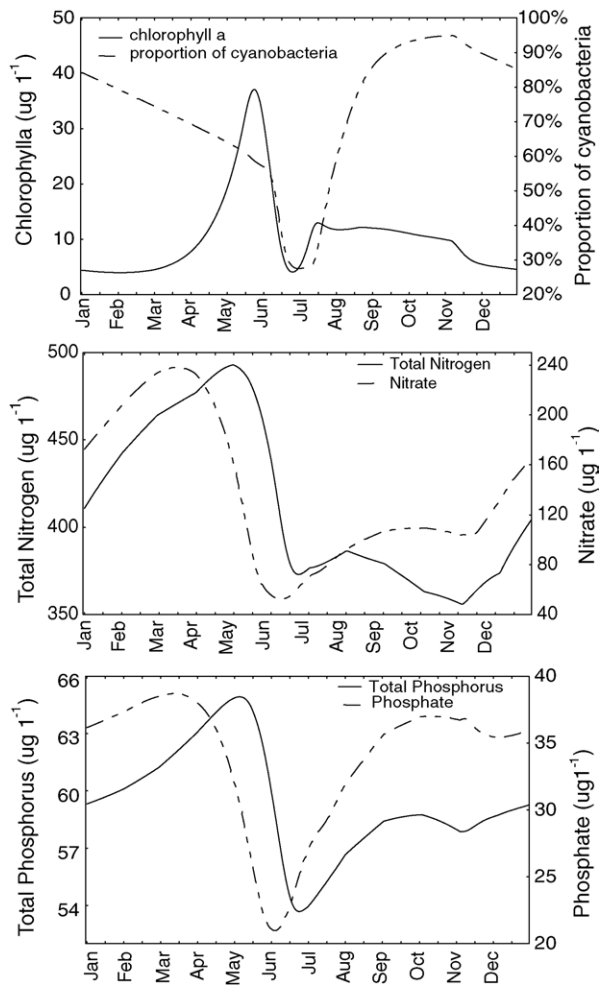

Fig. 8. Simulated epilimnetic chlorophyll, proportion of cyanobacteria, PO$_4$, TP, NO$_3$ and TN annual cycles, based on nutrient loadings from the year 1962. Nutrient concentrations are averages weighted over the epilimnion and hypolimnion volume.

values during 1962. These discrepancies probably result from a mis-characterization of sediment nitrate and ammonium fluxes. The likelihood that nitrification is mostly localized to the sediments of deep freshwater systems was also discussed by Pauer and Auer (2000), but the differences between their study system (Lake Onondaga, NY) and Lake Washington along with the lack of relevant data for Lake Washington make it inappropriate to adopt their high sediment–water interface nitrification rates (0.21–0.42 g m^{-2} day^{-1}). [Note that higher sediment nitrification rates would have also

improved the underestimation of the current summer hypolimnetic nitrate.]

The inclusion of both zooplankton groups in the simulations resulted in a lower spring phytoplankton maximum ($17 \mu g \, chl \, l^{-1}$) and two lower peaks ($10 \mu g \, chl \, l^{-1}$) during the summer and early fall period. Cyanobacteria still dominated the phytoplankton community, but their proportion varied between 40 and 50%. The summer-early fall phosphate and nitrate patterns were also dependent on the phytoplankton–zooplankton oscillations. The model overestimated total nitrogen concentrations, which was an effect of increased nitrogen egestion during cladoceran feeding. A desirable model outcome would have been the extinction or at least a significant decrease in cladoceran biomass, reflecting the filter-feeder sensitivity to increasing concentrations of the lower quality food-type (cyanobacteria). One explanation for why this did not happen is that our gross growth-efficiency parameterization is primarily driven by the food concentrations. The weighting scheme and more specifically the calibration $FQ_{(cyan,j)}$ value is probably sufficient for describing the food quality of the currently dominant cyanobacteria genera of Lake Washington, but is not representative for past conditions. During the prediversion period, *Oscillatoria rubescens* dominated the phytoplankton community, which inhibited consumption of edible phytoplankton by *Daphnia* by mechanical interference of the feeding apparatus (Infante and Abella, 1985). The existing formulations used in our model do not directly account for such feeding interference, or at least this cannot be obtained with the prescribed range (0–1) for the FQ index. Within the present modeling framework, the potential impact of mechanical feeding interference by filamentous cyanobacteria can be explored by assigning negative $FQ_{(cyan,j)}$ values. For example, when the system was forced with the 1962 nutrient loadings and a $FQ_{(cyan,j)} = -0.8$, the spring phytoplankton maximum was nearly $30 \mu g \, chl \, l^{-1}$ and the summer phytoplankton–zooplankton oscillations were significantly dampened. In addition, the cladoceran biomass was notably (>40%) lower and the proportion of cyanobacteria increased to a range of 50–70%. Finally, it should be noted that more successful reproductions of ecosystem adaptations and shifts in plankton community composition were obtained in the lake modeling literature with structural dynamic approaches (Zhang et al., 2003a,b, 2004). By replacing the rigid structure of the classic aquatic biogeochemical models with continuously changing parameter values, this strategy has provided satisfactory simulation results of system dynamics under variant environmental conditions. Thus, this alternative framework warrants consideration for getting reliable parameter estimates and more effectively featuring ecosystem response to perturbations.

4.2. Scenarios analysis

We used the Lake Washington eutrophication model to explore possible ecosystem structural shifts that might be induced by two alternative management scenarios relative to current simulated lake dynamics. The two scenarios involved increased nutrient loading equivalent to 25% of the 1962 point source loading levels (point loading$_{sc1,2} = 0.25 \times 1962$ point loading). In the first case, the sewage treatment plant effluents were discharged exclusively to the hypolimnion (scenario 1), and in the second scenario these effluents were discharged equally between the epilimnion and hypolimnion. In the first loading scenario, most of the incoming nutrients would not be directly available to phytoplankton uptake until fall mixing when physical conditions (light, temperature) are not favorable for phytoplankton growth. The second scenario considers nutrient supply to the epilimnion during the summer-stratified period, when the phytoplankton community is nutrient limited and more susceptible to cyanobacteria dominance. The system dynamics were studied through a variety of meteorological conditions (temperature, solar radiation, precipitation). In contrast with Part I, the present analysis considered both intra- and interannual variability, by introducing perturbations to the monthly values for the model forcing functions. For example, a simulated year with an unusually cold and wet May (deeper epilimnion, increased fluvial nutrients, lower water temperatures and reduced solar radiation) could be followed by a June with the opposite characteristics. Based on individual month variability, we formed 150 sets (annual cycles) of meteorological forcing that were used for identifying structural shifts in the lake patterns between the three nutrient loading scenarios.

Summary statistics for the annual values for the epilimnetic phytoplankton biomass, proportion of cyanobacteria, TN, NO_3, TP, and PO_4 are presented

Table 2
Monte Carlo analysis of the model based on current nutrient loading conditions and the two scenarios of increased nutrient loading

	Phytoplankton biomass	Proportion of cyanobacteria	Total nitrogen	Nitrate	Total phosphorus	Phosphate
Current conditions						
Mean	199	21	354	171	17.2	7.4
Standard deviation	13	2	53	32	1.9	1.4
Maximum	234	25	470	237	22.9	11.6
Minimum	171	15	249	111	12.9	4.5
Scenario 1						
Mean	244	27	346	144	23.7	10.8
Standard deviation	10	2	54	31	2.8	2.1
Maximum	273	35	465	210	32.2	16.5
Minimum	222	22	243	89	17.6	6.6
Scenario 2						
Mean	252	28	346	138	24.3	10.9
Standard deviation	13	3	53	27	2.9	2.1
Maximum	292	40	463	196	33.1	16.9
Minimum	224	24	243	89	18.1	6.6

Summary statistics of the annual values of the epilimnetic phytoplankton biomass ($\mu g\, C\, l^{-1}$), proportion of cyanobacteria (%), total nitrogen ($\mu g\, N\, l^{-1}$), nitrate ($\mu g\, N\, l^{-1}$), total phosphorus ($\mu g\, P\, l^{-1}$), and phosphate ($\mu g\, P\, l^{-1}$).

in Table 2. Both nutrient loading scenarios resulted in an increase of the mean annual phytoplankton biomass of about 40–50 $\mu g\, C\, l^{-1}$, and an epilimnetic cyanobacteria proportion that was 6–7% higher than the current level. In addition, there were simulated years for the second scenario (effluents distributed between epilimnion and hypolimnion), when epilimnetic cyanobacteria comprised an average of 38–40% of the phytoplankton community and their proportion during the summer-stratified period exceeded 50%. There was also a decreasing trend for epilimnetic nitrogen, and especially NO_3 concentrations which was about 10% lower than current conditions. In contrast, annual TP and PO_4 concentrations increased on average by 6 and 3 $\mu g\, P\, l^{-1}$. It should be noted, however, that phosphorus was still the limiting nutrient. Under the enrichment scenarios the system was characterized by larger spring phytoplankton blooms ($\approx$15 $\mu g\, chl\, l^{-1}$), and more frequent late summer-early fall secondary blooms ($\approx$5−10 $\mu g\, chl\, l^{-1}$).

We further explored the simulated epilimnetic phytoplankton patterns by applying principal component analysis to a matrix of 12 (months of the year) and 150 rows (simulated years). The basic rational behind this application of PCA is that different phases of the intra-annual cycle are driven by different mechanisms and may behave independently of each other, thus im-

peding identification of clear cause-effect relationships (Jassby, 1999). Selection of significant principal components (modes of variability) was based on the Monte Carlo technique "Rule N" (Overland and Preisendorfer, 1982), and significant modes were rotated using the normalized varimax strategy (Richman, 1986). The PCA results were nearly identical between the current conditions and two nutrient loading scenarios. Three significant principal components accounted for about 94% of the total variance; correlation coefficients between the individual months and the principal components are presented in Table 3. The first mode was most closely associated with November, December, January and May. The months June–October were most strongly loaded on the second mode, while the third mode was associated with February–April conditions. October was almost equally loaded on the first and second principal components. The second mode describes phytoplankton dynamics during the thermally stratified period. The third mode is associated with the period when light-limiting conditions recede, thereby triggering the spring phytoplankton bloom. The first mode primarily reflects the winter period when light levels limit phytoplankton growth. However, the inclusion of May in this mode is perplexing. During this month, the system is probably driven by all of the factors (mostly temperature) that regulate cladoceran biomass which

Table 3
Monte Carlo analysis of the model based on current nutrient loading conditions and two scenarios of increased nutrient loading

Months	Current conditions			Scenario 1			Scenario 2		
	First mode (36%)	Second mode (30%)	Third mode (29%)	First mode (36%)	Second mode (27%)	Third mode (31%)	First mode (36%)	Second mode (27%)	Third mode (30%)
January	**0.932**	−0.124	0.310	**0.926**	−0.291	0.080	**0.876**	−0.325	0.277
February	0.039	−0.228	**0.938**	−0.579	−0.021	**0.797**	−0.518	−0.076	**0.831**
March	−0.423	−0.078	**0.876**	−0.662	0.085	**0.729**	−0.644	0.048	**0.747**
April	−0.150	0.041	**0.920**	−0.259	0.026	**0.925**	−0.257	0.012	**0.909**
May	**0.859**	0.189	−0.343	**0.883**	−0.099	−0.419	**0.904**	−0.026	−0.390
June	−0.019	**0.752**	−0.481	−0.452	**0.668**	−0.379	−0.445	**0.684**	−0.352
July	−0.343	**0.788**	0.456	−0.206	**0.825**	0.427	−0.104	**0.861**	0.383
August	0.291	**0.898**	−0.199	−0.256	**0.877**	−0.303	−0.226	**0.891**	−0.251
September	0.242	**0.966**	0.023	0.181	**0.929**	0.015	0.399	**0.856**	−0.080
October	0.651	0.660	−0.340	0.577	0.618	−0.455	0.591	0.626	−0.446
November	**0.912**	0.263	−0.303	**0.959**	0.021	−0.239	**0.969**	0.045	−0.199
December	**0.975**	0.094	−0.187	**0.955**	−0.226	0.063	**0.968**	−0.184	0.071

Component coefficients ($n = 150$) for the principal components extracted from the PCA of the simulated epilimnetic phytoplankton biomass. Months with significant loadings, which also form the respective modes of variability, are indicated with bold numbers.

is the dominant grazer and strongly controls the phytoplankton standing crop.

Based on averages over the months for each of the three independent modes of variability, we computed a correlation matrix between the epilimnetic phytoplankton biomass and water temperature; TN, NO_3, TP, and PO_4 concentrations, total zooplankton, cladoceran and copepod biomass (Table 4). The strong negative correlation coefficients between water temperature ($r < −0.880$), cladoceran biomass ($r < −0.820$) and epilimnetic phytoplankton biomass support the previous explanation about the ecological processes that drive the first mode of variability. In addition, cladocerans depress phytoplankton biomass during the summer-stratified period ($r < −0.500$), but respond positively to the spring bloom ($r > 0.730$). Significant positive correlations between phytoplankton and copepod biomass were observed during most of the annual cycle, which suggests copepod grazing will not depress phytoplankton biomass given the model configuration and the coefficients selected. The strong positive correlation coefficients between phytoplankton biomass, and TP ($r > 0.815$) and PO_4 ($r > 0.828$) during the third mode (February–April) suggest the importance of phosphorus concentrations for spring bloom development. Generally, the phytoplankton correlations with the remaining environmental variables over the three modes were unaffected by the two nutrient enrichment scenarios. Interesting trends were

found between phytoplankton, and TP and PO_4 during the summer-stratified period (second mode). The positive correlation coefficients between phytoplankton biomass and TP ($r > 0.315$) indicate that due to the low summer phosphorus levels (relative to the assigned $KP_{(i)}$ values) the phytoplankton responds to concentration changes, and therefore most of the available phosphorus is sequestered in phytoplankton cells. During the present phosphorus-limiting conditions, this results in a negative correlation between algal biomass and PO_4 ($r = −0.267$, $p = 0.001$) which however is dampened and becomes insignificant for the first ($r = 0.009$, $p = 0.916$) and second ($r = −0.069$, $p = 0.403$) nutrient loading scenarios. This relaxation in phosphorus-limitation during the summer-stratified period was more evident between cyanobacteria biomass, and TP and PO_4 (Table 5). Being the weakest phosphorus competitors, cyanobacteria benefit less from the small increases in phosphorus concentrations, which are primarily due to the meteorological forcing impacts on thermal stratification and external loading. Hence, under current conditions the correlation for cyanobacteria is non-significant ($r = −0.106$, $p = 0.196$) with TP and significantly negative ($r = −0.551$, $p < 0.001$) with PO_4. However, phosphorus supplied to Lake Washington in the two enrichment scenarios caused cyanobacteria biomass to increase. Consequently, the cyanobacteria correlation with TP increased significantly for both the first ($r = 0.170$, $p = 0.037$) and sec-

Table 4
Monte Carlo analysis of the model based on current nutrient loading conditions and two scenarios of increased nutrient loading

	Water temperature	Total nitrogen	Nitrate	Total phosphorus	Phosphate	Zooplankton	Cladocerans	Copepods
Current conditions								
First mode	−0.886 (<0.001)	0.750 (<0.001)	0.709 (<0.001)	−0.504 (<0.001)	−0.756 (<0.001)	−0.272 (0.001)	−0.820 (<0.001)	0.946 (<0.001)
Second mode	−0.273 (0.001)	0.526 (<0.001)	0.392 (<0.001)	0.315 (<0.001)	−0.267 (0.001)	0.176 (0.031)	−0.512 (<0.001)	0.480 (<0.001)
Third mode	0.801 (<0.001)	−0.229 (0.005)	−0.319 (<0.001)	0.849 (<0.001)	0.829 (<0.001)	0.859 (<0.001)	0.737 (<0.001)	0.882 (<0.001)
Scenario 1								
First mode	−0.932 (<0.001)	0.710 (<0.001)	0.549 (<0.001)	−0.708 (<0.001)	−0.860 (<0.001)	−0.318 (<0.001)	−0.874 (<0.001)	0.888 (<0.001)
Second mode	0.174 (0.033)	0.070 (0.396)	−0.082 (0.321)	0.494 (<0.001)	0.009 (0.916)	−0.255 (0.002)	−0.751 (<0.001)	0.088 (0.286)
Third mode	0.906 (<0.001)	−0.518 (<0.001)	−0.571 (<0.001)	0.849 (<0.001)	0.851 (<0.001)	0.894 (<0.001)	0.826 (<0.001)	0.911 (<0.001)
Scenario 2								
First mode	−0.931 (<0.001)	0.729 (<0.001)	0.513 (<0.001)	−0.593 (<0.001)	−0.825 (<0.001)	−0.246 (0.002)	−0.870 (<0.001)	0.915 (<0.001)
Second mode	0.040 (0.624)	0.187 (0.022)	−0.002 (0.976)	0.443 (<0.001)	−0.069 (0.403)	−0.084 (0.305)	−0.678 (<0.001)	0.244 (0.003)
Third mode	0.870 (<0.001)	−0.422 (<0.001)	−0.473 (<0.001)	0.815 (<0.001)	0.828 (<0.001)	0.867 (<0.001)	0.795 (<0.001)	0.839 (<0.001)

Correlation matrix between the epilimnetic phytoplankton biomass and water temperature, total nitrogen, nitrate, total phosphorus, phosphate, total zooplankton, cladocerans and copepods biomass. The correlation coefficients ($n = 150$) were computed for each mode of variability based on averages over the respective months.

Table 5
Monte Carlo analysis of the model based on current nutrient loading conditions and two scenarios of increased nutrient loading

	Water temperature	Total nitrogen	Nitrate	Total phosphorus	Phosphate	Zooplankton	Cladocerans	Copepods
Current conditions								
First mode	−0.245 (0.003)	0.600 (<0.001)	0.523 (<0.001)	0.081 (0.326)	−0.187 (0.022)	0.397 (<0.001)	0.089 (0.277)	0.763 (<0.001)
Second mode	−0.774 (<0.001)	0.854 (<0.001)	0.807 (<0.001)	−0.106 (0.196)	−0.551 (<0.001)	0.750 (<0.001)	0.000 (0.996)	0.885 (<0.001)
Third mode	0.773 (<0.001)	−0.108 (0.190)	−0.205 (0.012)	0.863 (<0.001)	0.807 (<0.001)	0.857 (<0.001)	0.737 (<0.001)	0.872 (<0.001)
Scenario 1								
First mode	−0.549 (<0.001)	0.572 (<0.001)	0.394 (<0.001)	−0.417 (<0.001)	−0.580 (<0.001)	0.160 (0.051)	−0.503 (<0.001)	0.916 (<0.001)
Second mode	−0.273 (0.001)	0.416 (<0.001)	0.293 (<0.001)	0.170 (0.037)	−0.273 (0.001)	0.153 (0.061)	−0.693 (<0.001)	0.482 (<0.001)
Third mode	0.942 (<0.001)	−0.490 (<0.001)	−0.543 (<0.001)	0.896 (<0.001)	0.898 (<0.001)	0.951 (<0.001)	0.920 (<0.001)	0.875 (<0.001)
Scenario 2								
First mode	−0.591 (<0.001)	0.655 (<0.001)	0.442 (<0.001)	−0.270 (0.001)	−0.529 (<0.001)	0.217 (0.008)	−0.525 (<0.001)	0.940 (<0.001)
Second mode	−0.231 (<0.001)	0.393 (<0.001)	0.225 (0.006	0.323 (<0.001)	−0.131 (0.110)	0.163 (0.047)	−0.569 (<0.001)	0.457 (<0.001)
Third mode	0.910 (<0.001)	−0.411 (<0.001)	−0.457 (<0.001)	0.876 (<0.001)	0.902 (<0.001)	0.924 (<0.001)	0.903 (<0.001)	0.763 (<0.001)

Correlation matrix between the epilimnetic cyanobacteria biomass and water temperature, total nitrogen, nitrate, total phosphorus, phosphate, total zooplankton, cladocerans and copepods biomass. The correlation coefficients ($n = 150$) were computed for each mode of variability based on averages over the respective months.

ond ($r = 0.323$, $p < 0.001$) scenarios. This is also evident for PO_4 in the first ($r = -0.273$, $p < 0.001$) and second ($r = -0.131$, $p = 0.110$) scenarios. [Note that with the second scenario the correlation coefficient becomes non-significant, due to the constant discharge of nutrients to the epilimnion during the stratified period.]

Finally, we tested the system's resilience to disturbances that resemble episodic mixing events during the summer-stratified period. We induced a wide variety of pulses, i.e., continuous/semi-continuous, moderate/high frequency (8–365 year^{-1}), and low/high amplitude ($K = 0.17$–0.80 m^2 day^{-1}) under the three nutrient scenarios. Generally, the planktonic ecosystem did not show major structural shifts due to nutrient pulses from hypolimnetic intrusions. As was expected, the highest summer phytoplankton peaks (6–8 μg chl l^{-1}) were observed with the two enrichment scenarios, and these increases were proportionally allocated between the three phytoplankton groups. There are several factors that can affect the outcome of species competition in the summer epilimnion, i.e., concentrations of the three phytoplankton groups and phosphate levels at the onset of the thermal stratification, herbivorous grazing and also the hydrodynamic regime in the epilimnion. These factors dynamically regulate the growth-minus-loss balance for each phytoplankton group and determine the "superior" competitor under any specific set of conditions (Grover, 1991). Transient nutrient pulses are thought to induce competitive advantages for "storage strategists", such as the group that was labeled "cyanobacteria" in the present model (Suttle et al., 1987; Grover, 1991). The aforementioned results resemble those obtained, when the model was forced with 1962 nutrient loadings and both zooplankton groups were activated. The explanation is probably similar and is associated with the presence of the dominant grazers (cladocerans) which act as a "safety valve" and do not allow cyanobacteria to gain a competitive advantage. An additional condition is necessary to relax the cyanobacteria competitive handicap in the phosphorus limited-environment of the summer epilimnion. Prevailing physical (turbulence) conditions could probably provide an additional support, but the reproduction of their role is not feasible with the present model's simplified physical structure.

Since wastewater was diverted from Lake Washington in the late 1960s a major cyanobacteria bloom has only occurred once. This event invoked questions about the stability of the present trophic status and the possibility that Lake Washington might again shift towards cyanobacteria dominance. In agreement with inferences above, Edmondson (1997) suggested high wind velocities most likely promoted the 1988 *Aphanizomenon* bloom. He claimed strong and continuous summer winds caused greater water column mixing, which in turn might have been the reason why *Aphanizomenon* colonies were distributed throughout the epilimnion and did not solely accumulate at the surface. Moreover, the physiological literature suggests *Aphanizomenon* has excellent nutrient storage capacities, and can therefore gain a competitive advantage due to pulsed nutrient supplies (Uehlinger, 1981; De Nobel et al., 1997). Probably a coincidental combination of a favorable fine-scale hydrodynamic environment with an unstable mixing depth (Edmondson, 1997 Fig. 17), associated with transient nutrient pulses enabled *Aphanizomenon* to outcompete *Microcystis*, *Anabaena*, *Fragilaria* and *Cryptomonas* (the usual mid- and late summer genera in Lake Washington), which also have a higher P-affinity and higher maximum growth rates (Sommer, 1985; Sommer, 1989; Grover, 1991). The coupling of the present eutrophication model with a hydrodynamic model with appropriate resolution will make it possible to simulate similar conditions and test this hypothesis.

5. Future modifications and conclusions

Our eutrophication model provided a good representation of the key epilimnetic and hypolimnetic patterns in Lake Washington (USA). A satisfactory fit was obtained between simulated and observed monthly values and the relative error was below 20% for the major water quality parameters (phytoplankton, phosphate, total phosphorus, total nitrogen, dissolved oxygen). Furthermore, the model was forced by the 1962 nutrient loadings (when the lake received the maximum input of secondary sewage effluents) and accurately predicted the phytoplankton response (chlorophyll levels, cyanobacteria dominance) and the nitrogen and phosphorus annual cycles. However, several issues were raised during model calibration and validation that should guide model modifications and future research on this lake.

- The model computed greater phosphate and ammonium accumulation in the hypolimnion during the

stratified period than was actually observed. This was most likely caused by the simple physical segmentation (epilimnion/hypolimnion) of the model which did not allow for heterogeneity within the spatial compartments. For example, the sediment fluxes are instantaneously diluted over the entire hypolimnion volume and the vertical temperature profiles are constant from the thermocline to bottom. Considering the model sensitivity to parameters related to the temperature-dependence of biochemical processes (Part I) along with the increasing sediment nutrient release rates during the summer, it can be inferred that a multi-layer vertical characterization of the system is important for simulating the hypolimnetic vertical profiles during the stratified period. Although, our explicitly prescribed mixed-layer monthly variations were based on the lake's measured vertical profiles, they cannot represent the micro- and macroscale physical processes in the water column. This is particularly important for large lakes such as Lake Washington, where water circulation is the combined effect of several factors e.g., river inflows, bottom friction, bathymetry, barometric pressure changes, convective currents due temperature differences between the inflows and the lake and wind action on the water surface that can cause surface seiches and internal waves (Johnson et al., 2003). The integration with a hydrodynamic component will also make it possible to test several hypotheses about lake dynamics, e.g, the initiation of the spring bloom based on incomplete vertical mixing patterns (the so-called "critical turbulence concept" by Huisman et al., 1999) or the possible role of fine-scale hydrodynamic processes for species competition (the 1988 *Aphanizomenon* bloom event).

- As previously discussed, inclusion of independent zooplankton C, N and P efficiencies, to maintain constant somatic elemental ratios, increased the influence of the non-limiting element recycling on the model outputs. A characteristic example was the sensitivity of the simulated nitrogen cycle to plankton basal metabolism and the zooplankton egestion fractionation. The adoption of a higher dissolved phase fraction (DON and NH_4) increased the ammonium concentrations to much higher levels than those observed in the system. During the calibration, we pursued several approaches to solve this problem, i.e., increased ammonium inhibition to nitrate

uptake (ψ values), lowered remineralization rates ($KNref_{dissolution}$, $KNref_{mineral}$) and increased nitrification rates ($nitrif_{max}$). None of these approaches proved to be more effective than simply assuming a higher particulate fraction during nitrogen recycling. This partitioning corresponds to the hypothesis that zooplankton homeostasis is also maintained during the digestion and assimilation process, i.e., by removing elements in proportion to zooplankton body ratios as opposed to the elemental ratio of the food (Elser and Foster, 1998). A particulate fraction of 65% resulted in sedimentation rates that were within the observed ranges from past studies of Lake Washington (Edmondson and Lehman, 1981). However, the fact that these observations only partially overlap with the period when *Daphnia* became a dominant component of the zooplankton community, indicates that further research is required to verify these rates and probably a higher particulate fraction would be more appropriate for simulating downward nitrogen fluxes during current conditions. Increased nitrogen sedimentation and accumulation to the lake bottom might have also changed the relative magnitudes of the various sediment processes. For example, the model results showed increased nitrification rates improved the agreement between simulated and observed hypolimnetic nitrate concentrations during both the calibration and validation periods. If the simulated nitrate deficit is actually a result of increased nitrification (sediments or water column) which is unaccounted for by the model, this needs to be supported by field data. Moreover, greater particulate deposition rates might have promoted sediment denitrification, which in turn can – at least in part – explain the significant alkalinity increase in the lake (Edmondson, 1994, Fig. 2E). Kuivila and Murray (1984) indicated that denitrification occurred near the sediment–water interface, but considered denitrification's contribution to alkalinity small compared with the other organic matter diagenesis processes. This study provided evidence that rapid reactions taking place at the lake sediment interface were an important source of alkalinity. Their pore-water estimates varied from 0.69 to 3.95 equiv. $m^{-2} day^{-1}$, and Kuivila and Murray (1984) also reported estimates of late summer-early fall alkalinity fluxes of 8.2 equiv. $m^{-2} day^{-1}$ that cannot be accounted for by river inputs. This deviates from Edmondson's (1994)

hypothesis that the observed lake water alkalinity increases were most likely induced by land-cover changes in the watershed that altered chemical inputs to streams. Whether the relative magnitudes of nitrification/denitrification have changed in the lake after the resurgence of P-rich *Daphnia* and their net effect (decrease of alkalinity by nitrification and increase by denitrification) can be associated with the observed alkalinity patterns, are issues that can be investigated in the current lake sampling program.

- Finally, our primary focus in the present model calibration was to constrain the parameters through a description of observed lake dynamics, and then test the model's utility, (i) as a heuristic tool for exploring the internal structure of the simulated C, N, P cycles, and (ii) as a predictive tool for simulating likely nutrient enrichment responses. The final model calibration will also include the hydrodynamic and fish-bioenergetic components. The application of optimization techniques can provide an essential aid at this stage. A wide variety of techniques designed to identify both local and global minima have been developed over the last decade in aquatic system models (e.g., Matear, 1995; Hurtt and Armstrong, 1999; Vallino, 2000; Atthias et al., 2000). The richness of the Lake Washington database is also an excellent opportunity for applying data assimilation schemes which provide dynamically consistent solutions with both observations and model equations (Doney, 1999). The control for the growth of prediction errors, the more accurate estimates of models parameters (including initial and boundary conditions, forcing functions) that can result by their application will also increase the model's value as a management tool. Even though data assimilation for coupled biological-physical processes can be complicated (Gregoire et al., 2003), and implementations to three-dimensional models are more limited (Matear and Holloway, 1995), the available information for Lake Washington is a promising starting point.

References

Ambrose, R.B., Martin, J.L., Connolly, J.P., Schanz, R.W., 1991. WASP4, a hydrodynamic and water quality model. Model theory user's manual and programmer's guide, Environmental Protection Agency, Athens, GA, EPA 600: 3-86-034.

Arhonditsis, G., Tsirtsis, G., Angelidis, M., Karydis, M., 2000. Quantification of the effects of nonpoint nutrient sources to coastal marine eutrophication: applications to a semi-enclosed gulf in the Mediterranean Sea. Ecol. Model. 129, 209–227.

Arhonditsis, G., Karydis, M., Tsirtsis, G., 2002. Integration of mathematical modeling and multicriteria methods in assessing environmental change in developing areas: a case study of a coastal system. J. Coastal. Res. 18, 698–711.

Arhonditsis, G., Brett, M.T., Frodge, J., 2003. Environmental control and limnological impacts of a large recurrent spring bloom in Lake Washington, USA. Environ. Manage. 31, 603–618.

Arhonditsis, G.B., Brett, M.T., 2004. Evaluation of the current state of mechanistic aquatic biogeochemical modelling. Mar. Ecol-Prog. Ser. 271, 13–26.

Atthias, V., Massega, P., Jeandel, C., 2000. Selecting a global optimization method to estimate the oceanic particle cycling rate constants. J. Mar. Res. 58, 675–707.

Ballantyne, A.P., Brett, M.T., Müller-Navarra, D.C. Biochemical control of herbivorous zooplankton growth: *Daphnia pulex* responses to natural seston composition, submitted for publication.

Beauchamp, D.A., 1996. Estimating the Carrying Capacity for Planktivorous Fishes in Lake Washington. Washington Department of Fisheries and Wildlife.

Boyd, P.W., Doney, S.C., 2002. Modeling regional responses by marine pelagic ecosystems to global climate change. Geophys. Res. Lett. 29, Art. No. 1806.

Brett, M.T., Arhonditsis, G.B., Mueller, S.E., Hartley, D.M., Frodge, J.D., Funke, D.E. Non point source impacts on stream nutrient concentrations along a forest to urban gradient. Environ. Manage., in press.

Caswell, H., 1976. The validation problem. In: Patten, B. (Ed.), System Analysis and Simulation in Ecology, vol. IV. Academic Press, New York, pp. 313–325.

Caswell, H., 1988. Theory and models in ecology: a different perspective. Ecol. Model. 43, 33–44.

Cerco, C.F., Cole, T.M., 1994. CE-QUAL-ICM: a three-dimensional eutrophication model, version 1.0. User's Guide, US Army Corps of Engineers Waterways Experiments Station, Vicksburgh, MS.

De Nobel, W.T., Huisman, J., Snoep, J.L., Mur, L.R., 1997. Competition for phosphorus between the nitrogen-fixing cyanobacteria Anabaena and Aphanizomenon. FEMS Microbiol. Ecol. 24, 259–267.

Devol, A.H., Packard, T.T., 1978. Seasonal-changes in respiratory enzyme-activity and productivity in Lake Washington microplankton. Limnol. Oceanogr. 23, 104–111.

Doney, S.C., 1999. Major challenges confronting marine biogeochemical modeling. Global Biogeochem. Cycles 13, 705–714.

Downing, J.A., Rigler, F.H., 1984. A Manual on Methods for the Assessment of Secondary Productivity in Fresh Waters, second ed. Blackwell Scientific Publications, Oxford, UK, 501 pp.

Edmondson, W.T., 1994. Sixty years of Lake Washington: a curriculum vitae. Lake Reserv. Manage. 10, 75–84.

Edmondson, W.T., 1997. Aphanizomenon in Lake Washington. Arch. Hydrobiol. 107 (Suppl.), 409–446.

Edmondson, W.T., Lehman, J.T., 1981. The effect of changes in the nutrient income on the condition of Lake Washington. Limnol. Oceanogr. 26, 1–29.

Elser, J.J., Foster, D.K., 1998. N:P stoichiometry of sedimentation in lakes of the Canadian shield: relationships with seston and zooplankton elemental composition. Ecoscience 5, 56–63.

Elser, J.J., Urabe, J., 1999. The stoichiometry of consumer-driven nutrient recycling: theory, observations, and consequences. Ecology 80, 735–751.

Fasham, M.J.R., Sarmiento, J.L., Slater, R.D., Ducklow, H.W., Williams, R., 1993. Ecosystem behavior at Bermuda station-S and ocean weather station India—a general circulation model and observational analysis. Global Biogeochem. Cycles 7, 379–415.

Franks, P.J.S., 1995. Coupled physical-biological models in oceanography. Rev. Geophys. 33, 1177–1187.

Frost, B.W., Kishi, M.J., 1999. Ecosystem dynamics in the eastern and western gyres of the Subarctic Pacific—a review of lower trophic level modeling. Prog. Oceanogr. 43, 317–333.

Gelda, R.K., Brooks, C.M., Effler, S.W., Auer, M.T., 2000. Interannual variations in nitrification in a hypereutrophic urban lake: occurrences and implications. Water Res. 34, 1107–1118.

Gregoire, M., Brasseur, P., Lermusiaux, P., 2003. The use of data assimilation in coupled hydrodynamic, ecological and bio-geochemical models of the ocean. 33rd International Liège Colloquium on Ocean Dynamics. J. Mar. Syst. 40–41, 1–3.

Grover, J.P., 1991. Resource competition in a variable environment—phytoplankton growing according to the variable-internal-stores model. Am. Nat. 138, 811–835.

Goodall, D.W., 1972. Building and testing ecosystem models. In: Jeffers, J.N.J. (Ed.), Mathematical Models in Ecology. Blackwell, Oxford, pp. 73–194.

Hamilton, D.P., Schladow, S.G., 1997. Prediction of water quality in lakes and reservoirs. 1. Model description. Ecol. Model. 96, 91–110.

Holling, C.S., 1978. Adaptive Environmental Assessment and Management. John Wiley and Sons, New York, 377 pp.

Huisman, J., Oostveen, P., Weissing, F.J., 1999. Critical depth and critical turbulence: two different mechanisms for the development of phytoplankton blooms. Limnol. Oceanogr. 44, 1781–1787.

Hurtt, G.C., Armstrong, R.A., 1999. A pelagic ecosystem model calibrated with BATS and OWSI data. Deep Sea Res. PT II 46, 27–61.

Infante, A., Abella, S.E.B., 1985. Inhibition of Daphnia by Oscillatoria in Lake Washington. Limnol. Oceanogr. 30, 1046–1052.

Jassby, A.D., 1999. Uncovering mechanisms of interannual variability from short ecological time series. In: Scow, K.M. (Ed.), Integrated Assessment of Ecosystem Health. CRC Press, pp. 285–306.

Johnson, B.H., Kim, S.C., Nail, G.H., 2003. A three-dimensional hydrodynamic and temperature model of Lake Washington. US Army Corps of Engineers Waterways Experiments Station, Vicksburgh, MS.

Jorgensen, S.E., 1995. The growth rate of zooplankton at the edge of chaos: ecological models. J. Theor. Biol. 175, 13–21.

Kamykowski, D., Yamazaki, H., Janowitz, G.S., 1994. A Lagrangian model of phytoplankton photosynthetic response in the upper mixed layer. Deep-Sea Res. 16, 059–069.

Kawamiya, M., 2002. Numerical model approaches to address recent problems on pelagic ecosystems. J. Oceanogr. 58, 365–378.

Kuivila, K.M., Murray, J.W., 1984. Organic-matter diagenesis in fresh-water sediments—the alkalinity and total CO_2 balance and methane production in the sediments of Lake Washington. Limnol. Oceanogr. 29, 1218–1230.

Kuivila, K.M., Murray, J.W., Devol, A.H., Lidstrom, M.E., Reimers, C.E., 1988. Methane cycling in the sediments of Lake Washington. Limnol. Oceanogr. 33, 571–581.

Lehman, J.T., 1988. Hypolimnetic metabolism in Lake Washington—relative effects of nutrient load and food web structure on lake productivity. Limnol. Oceanogr. 33, 1334–1347.

Lehman, J.T., 1978. Aspects of nutrient dynamics in freshwater communities. Ph.D. thesis. University of Washington.

Matear, R.J., 1995. Parameter optimization and analysis of ecosystem models using simulated annealing—a case study at station-P. J. Mar. Res. 53, 571–607.

Matear, R.J., Holloway, G., 1995. Modeling the inorganic phosphorus cycle of the North Pacific using an adjoint data assimilation model to assess the role of dissolved organic phosphorus. Global Biogeochem. Cycles 9, 101–119.

Mayer, D.G., Butler, D.G., 1993. Statistical validation. Ecol. Model. 68, 21–32.

Norberg, J., DeAngelis, D., 1997. Temperature effects on stocks and stability of a phytoplankton–zooplankton model and the dependence on light and nutrients. Ecol. Model. 95, 75–86.

Omlin, M., Brun, P., Reichert, P., 2001. Biogeochemical model of Lake Zürich: sensitivity, identifiability and uncertainty analysis. Ecol. Model. 141, 105–123.

Oreskes, N., Shrader-Frechette, K., Belitz, K., 1994. Verification, validation, and confirmation of numerical models in the earth-sciences. Science 263, 641–646.

Overland, J.E., Preisendorfer, R.W., 1982. A significance test for principal components applied to a cyclone climatology. Mon. Weather Rev. 110, 1–4.

Pauer, J.J., Auer, M.T., 2000. Nitrification in the water column and sediment of a hypereutrophic lake and adjoining river system. Water Res. 34, 1247–1254.

Power, M., 1993. The predictive validation of ecological and environmental models. Ecol. Model. 68, 33–50.

Quay, P.D., Emerson, S.R., Quay, B.M., Devol, A.H., 1986. The carbon-cycle for Lake Washington—a stable isotope study. Limnol. Oceanogr. 31, 596–611.

Reckhow, K.H., 1999. Water quality prediction and probability network models. Can. J. Fish. Aquat. Sci. 56, 1150–1158.

Richey, J.E., 1979. Patterns of phosphorus supply and utilization in Lake Washington and Findley Lake. Limnol. Oceanogr. 24, 906–916.

Richman, M.B., 1986. Rotation of principal components. J. Climatol. 6, 293–335.

Rinaldi, S., Muratori, S., 1993. Conditioned chaos in seasonally perturbed predator-prey. Ecol. Model. 69, 79–97.

Rykiel, E.J., 1996. Testing ecological models: the meaning of validation. Ecol. Model. 90, 229–244.

Scheffer, M., Rinaldi, S., Kuznetsov, Y.A., 2000. Effects of fish on plankton dynamics: a theoretical analysis. Can. J. Fish. Aquat. Sci. 57, 1208–1219.

Scheuerell, M.D., Schindler, D.E., Litt, A.H., Edmondson, W.T., 2002. Environmental and algal forcing of Daphnia production dynamics. Limnol. Oceanogr. 47, 1477–1485.

Schladow, S.G., Hamilton, D.P., 1997. Prediction of water quality in lakes and reservoirs. 2. Model calibration, sensitivity analysis and application. Ecol. Model. 96, 111–123.

Sommer, U., 1985. Comparison between steady state and non-steady state competition: experiments with natural phytoplankton. Limnol. Oceanogr. 30, 335–346.

Sommer, U., 1989. The role of competition for resources in phytoplankton succession. In: Sommer, U. (Ed.), Phytoplankton Ecology. Succession in Plankton Communities. Springer Verlag, pp. 57–106.

Straile, D., 1997. Gross growth efficiencies of protozoan and metazoan zooplankton and their dependence on food concentration, predator-prey weight ration, and taxonomic group. Limnol. Oceanogr. 42, 1375–1385.

Suttle, C.A., Stockner, J.G., Harrison, P.J., 1987. Effects of nutrient pulses on community structure and cell-size of a freshwater phytoplankton assemblage in culture. Can. J. Fish. Aquat. Sci. 44, 1768–1774.

Turner, R.K., 2000. Integrating natural and socio-economic science in coastal management. J. Marine. Syst. 25, 447–460.

Uehlinger, V.U., 1981. Experimental autecological studies of Aphanizomenon flos-aquae. Arch. Hydrobiol. 60, 260–288 (Algol Studies 28).

Vallino, J.J., 2000. Improving marine ecosystem models: use of data assimilation and mesocosm experiments. J. Mar. Res. 58, 117–164.

Van Horn, R.L., 1971. Validation of simulation results. Manage. Sci. 17, 247–258.

Zhang, J.J., Jorgensen, S.E., Tan, C.O., Beklioglu, M., 2003a. A structurally dynamic modelling—Lake Mogan, Turkey as a case study. Ecol. Model. 164, 103–120.

Zhang, J.J., Jorgensen, S.E., Beklioglu, M., Ince, O., 2003b. Hysteresis in vegetation shift—Lake Mogan prognoses. Ecol. Model. 164, 227–238.

Zhang, J.J., Jorgensen, S.E., Mahler, H., 2004. Examination of structurally dynamic eutrophication model. Ecol. Model. 173, 313–333.

Ziegler, B.P., 1976. Theory of Modeling and Simulation. John Wiley and Sons, New York, 435 pp.